

## HOW SPECIAL ARE BRIGHTEST CLUSTER GALAXIES? THE IMPACT OF NEAR-INFRARED LUMINOSITIES ON SCALING RELATIONS FOR BCGS

DAN BATCHELDOR<sup>1</sup>, ALESSANDRO MARCONI<sup>2</sup>, DAVID MERRITT<sup>3</sup> & DAVID J. AXON<sup>3</sup>

*ApJ Letters Accepted*

### ABSTRACT

Using the extended J, H and K magnitudes provided by the 2MASS data archive, we consider the position of brightest cluster galaxies (BCGs) in the observed relations between inferred supermassive black hole (SMBH) mass and the host galaxy properties, as well as their position in the stellar velocity dispersion and luminosity ( $\sigma_* - L$ ) relation, compared to E and S0 galaxies. We find that SMBH masses ( $M_\bullet$ ) derived from near-infrared (NIR) magnitudes do not exceed  $\sim 3 \times 10^9 M_\odot$  and that these masses agree well with the predictions made from  $\sigma_*$ . In the NIR, there is no evidence that BCGs leave the  $\sigma_* - L$  relation defined by less luminous galaxies. The higher SMBH masses predicted from V-band luminosities ( $M_\bullet \lesssim 10^{10.5} M_\odot$ ) are attributed to the presence of extended envelopes around the BCGs, however, this will need to be confirmed using deeper multiwavelength imaging.

*Subject headings:* galaxies: elliptical — galaxies: evolution — galaxies: fundamental parameters — galaxies: photometry

### 1. INTRODUCTION

Whether the first galaxies were formed from initial large-scale condensations, or grew from an assembly of smaller bodies, still remains one of the most fundamental questions in modern astrophysics. Studies of the most massive galaxies will provide important constraints on this. Similar considerations apply to supermassive black holes (SMBHs) as the masses of SMBHs correlate with properties of the host bulge (Ferrarese & Ford 2005), i.e., the SMBH mass *vs.* bulge luminosity ( $M_\bullet - L$ ) relation (Kormendy & Richstone 1995), the SMBH mass *vs.* stellar velocity dispersion ( $M_\bullet - \sigma_*$ ) relation (Ferrarese & Merritt 2000; Gebhardt et al. 2000), and the SMBH mass *vs.* Sérsic index relation (Graham & Driver 2007).

As highly luminous massive galaxies found toward the centers of galaxy clusters, brightest cluster galaxies (BCGs) have received considerable interest. The surface brightness profiles (SBPs) of BCGs are well fit by the same Sérsic (1963) law that describes less-luminous spheroids (Graham et al. 1996), apart from the outermost regions which sometimes exhibit faint, extended envelopes (Oemler 1976; Bernardi et al. 2006, hereafter B06). BCGs also appear to obey the same relations between fitting parameters that characterize E/S0 galaxies generally (Graham et al. 1996). Lauer et al. (2006, hereafter L06) noted that the  $M_\bullet - L$  relation, in the V-band ( $M_\bullet - L_V$ ), predicts higher SMBH masses in BCGs than are predicted by the  $M_\bullet - \sigma_*$  relation. B06 obtain similar results; the slope in the size-luminosity relation is found to be steeper in BCGs when compared to the bulk of E/S0's, and the  $\sigma_*$  *vs.* luminosity ( $\sigma_* - L_R$ ) relation is seen to flatten for the brightest galaxies.

While the low-scatter  $M_\bullet - \sigma_*$  relation is the pre-

ferred “secondary” SMBH mass estimation technique, compared to the larger-scatter  $M_\bullet - L_V$  relation, Marconi & Hunt (2003, hereafter MH03) have shown that the scatter in the relations become similar if parameters are derived in the near-infrared (NIR). With this in mind we have conducted a study of BCGs based on the 2MASS extended source catalog. We use the 219 L06 galaxies of which  $\sim 30\%$  are BCGs and the remainder are E/S0s. The L06 data include absolute V-band magnitudes ( $M_V$ ) and, except in 51 cases, a value for  $\sigma_*$ . We adopt the errors of 10% in  $M_V$  and  $\sigma_*$ , as quoted by L06. We supplement the  $M_V$  data with the NIR data contained within the 2MASS extended source catalog. All magnitudes are corrected for galactic extinction according to Schlegel et al. (1998). Distances are all adjusted to a common scale, with  $H_0 = 70 \text{ km s}^{-1} \text{ Mpc}^{-1}$ , and primarily taken from the survey of Tonry et al. (2001). Remaining distances are taken from Lainé et al. (2003) or from the Virgo in-fall corrected recessional velocities listed by Hyperleda<sup>4</sup> (Paturel et al. 2003). In § 2 we evaluate the 2MASS photometry. In § 3 we present the results, which are discussed in § 4. § 5 sums up.

### 2. 2MASS PHOTOMETRY

In this study we have used the 2MASS “total” magnitudes (e.g.,  $k_{m_{\text{ext}}}$ ) derived from SBP fitting extrapolation<sup>5</sup>, rather than aperture photometry which inevitably under-estimates the total galaxy magnitudes (Andreoni 2002). Briefly,  $k_{m_{\text{ext}}}$  is estimated by numerical integration of the Sérsic law, fitted between  $r > 7\text{--}10''$  (to avoid the point spread function) and the maximum radius ( $r_{\text{max}}$ ) of the SBP with a signal to noise greater than two. Assuming circular isophotes and  $r_{\text{max}} = 20\text{--}80''$  (see Figure 1), this corresponds to a SBP limit from 2.9 to 3.7 magnitudes below the 2MASS  $3\sigma$  limit (20.09, 19.34 and 18.55 in J, H and K). The best-fitting Sérsic law is then integrated up to  $r_{\text{ext}}$  (the galaxy “total” radius). Typically,  $r_{\text{ext}}$  is  $\sim 2\text{--}5$  times the radius of the 20

Electronic address: ddbpci@astro.rit.edu

<sup>1</sup> Center for Imaging Science, Rochester Institute of Technology, Rochester, NY 14623

<sup>2</sup> INAF-Osservatorio Astronomico Astrofisico di Arcetri, 50125 Firenze, Italy

<sup>3</sup> Department of Physics, Rochester Institute of Technology, Rochester, NY 14623

<sup>4</sup> <http://leda.univ-lyon1.fr>

<sup>5</sup> For more information see sections 2.3a and 4.5e of <http://www.ipac.caltech.edu/2mass/releases/allsky/doc/>

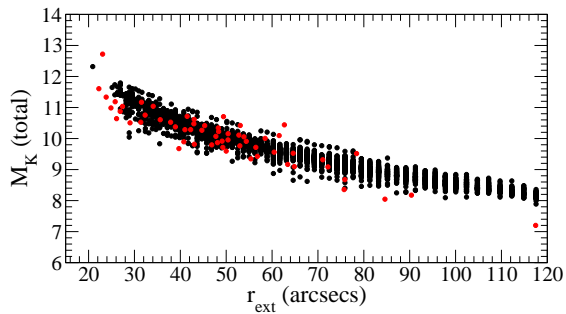


FIG. 1.— Simulations of 2MASS photometry. The distribution of simulated galaxy properties, total K-band magnitude and  $r_{\text{ext}}$ , (black circles) with respect to observed BCGs (red circles).

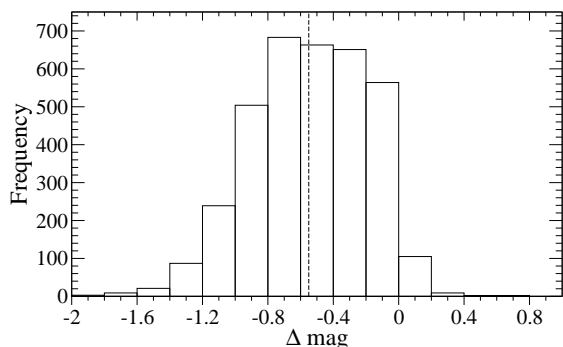


FIG. 2.— Simulations of 2MASS photometry. The difference between “true” and estimated magnitudes from  $\sim 3500$  simulations is shown. The dashed line marks the median of the distribution.

mag/arcsec<sup>2</sup> isophote (e.g.,  $r_{k20}$ ) where  $5 r_{k20}$  is imposed as a strict upper limit.

To quantify the importance of undetected light at large radii, we have carried out extensive simulations of BCGs and performed 2MASS analogous photometry. Over 3500 BCGs with  $M_V$  and  $z$  randomly distributed in the observed ranges ( $-24.5 - -22$  and  $0.015 - 0.050$ , respectively) were generated. For each BCG the effective radius was derived from the  $r_e - M_V$  relation provided by L06, and the Sérsic index,  $n$ , was derived from the  $n - r_e$  relation estimated from Figure 11 of Graham et al. (1996) (0.2 dex scatter was included for both). In all cases we imposed  $1 < n < 15$ . The observed total K magnitude,  $M_K$ , was then derived using  $V-K=3.6$ . The model images of each BCG (characterized by  $m_K$ ,  $r_e$  and  $n$ ) were then generated using GALFIT (Peng et al. 2002) to take into account the 2MASS pixel sizes ( $1''$ ) and spatial resolution (FWHM  $\sim 3''$ ). We added 2MASS typical noise ( $K = 19.74$  mag/arcsec<sup>2</sup> rms) and derived SBPs that were fitted with a Sérsic law to estimate  $r_{\text{ext}}$  and  $k-m_{\text{ext}}$ . To reproduce the magnitude-size relation (see Figure 1) we used an average  $r_{\text{ext}}$  of  $2.4 r_{k20}$ . Figures 1 and 2 show how the simulated magnitudes compare to the actual BCG magnitudes and the “true” simulated input magnitudes. The average offset is  $-0.5$  mags (50<sup>th</sup> percentile); 2MASS mildly underestimates  $M_K$  in BCGs. Simulations using bluer colors ( $V-K=3.3$ ) give very similar result.

In § 3 we will directly compare the results from extrapolating photometry estimated in the V-band and NIR. As the V-band photometry may have been gained from different radii (thereby gathering a different amount of light) we now briefly compare the relative sizes of the regions from which the photometry was derived.

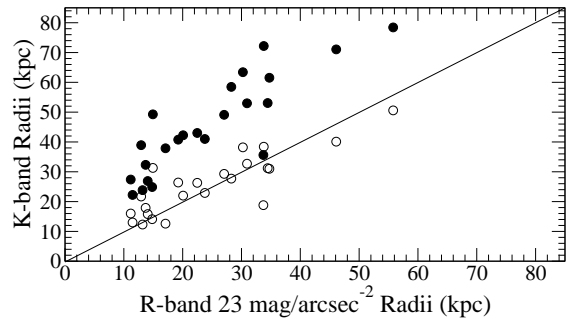


FIG. 3.— Comparing the radii of V-band and NIR magnitudes. The solid line is one-to-one. Open and closed circles show the relation between  $r_{r23}$  and  $r_{k20}$  and  $r_{\text{ext}}$  respectively.

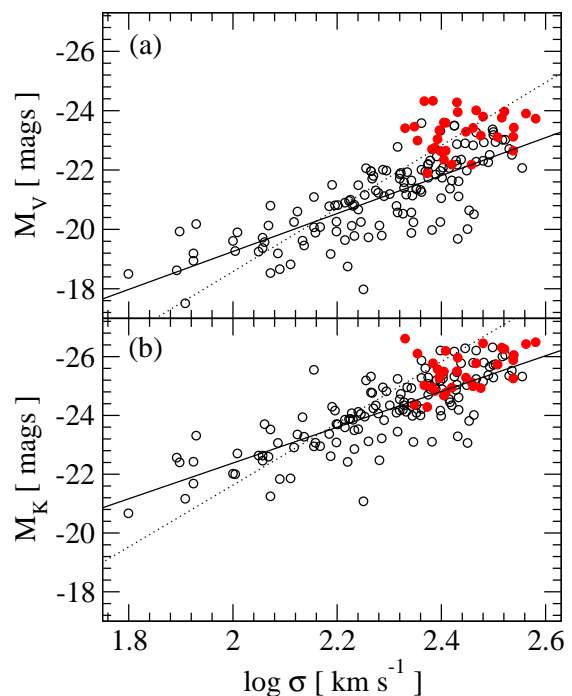


FIG. 4.— The relationship between  $\sigma_*$  and luminosity in the V-band (a) and K-band (b). Open black circles mark E and S0s, filled red circles show BCGs. The solid lines show the fit to just the E/S0s, the dotted lines mark the fit of Bernardi et al. (2006).

The L06 V-band BCG luminosities were provided by Laine et al. (2003), who in turn estimated the total magnitudes from SBPs presented by Postman & Lauer (1995). Graham et al. (1996) performed Sérsic fits to these SBPs using a limiting R-band surface brightness. Therefore, assuming a color of  $R-K=3.0$ , we can directly compare the radii of  $r_{\text{ext}}$  and  $r_{k20}$  (the radius of the  $K=20$  mag/arcsec<sup>2</sup> isophote) with the R-band surface brightness at  $23.0$  mag/arcsec<sup>2</sup> ( $r_{r23}$ ). By calculating  $r_{r23}$  from the Graham et al. (1996) BCG Sérsic fits, we find that  $r_{k20}$  agrees well with the  $r_{r23}$  radii (Figure 3). However,  $r_{\text{ext}}$  is always larger than  $r_{r23}$ . Therefore, the 2MASS magnitudes used in this study include light from at least as extended a region as the V-band magnitudes used by L06.

As an additional check, we can compare published values of  $M_K$  to those derived by MH03 from two-dimensional fitting to 2MASS profiles out to infinity. We find a systematic offset of  $\sim 0.4$  mags, consistent with our simulations.

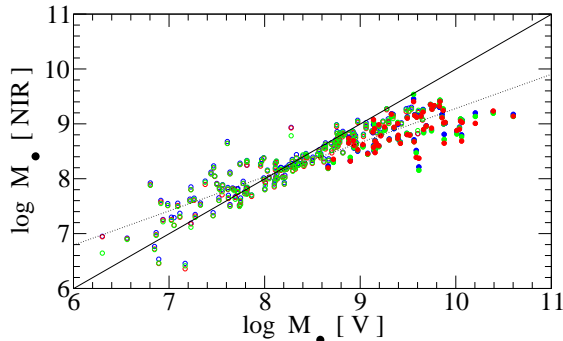


FIG. 5.— V-band *vs.* NIR  $M_{\bullet}$  estimates. The solid line marks a one-to-one relation. Open circles are E/S0s, closed circles are BCGs. Blue, green and red colors refer to the J, H and K bands respectively. The dotted line marks the fit to all the K-band data.

### 3. BCGS IN THE NIR

Figure 4 compares the  $\sigma_{*} - L_V$  and  $\sigma_{*} - L_K$  relations. In both cases we plot the best-fit relation defined by the E/S0 galaxies (solid line) as well as the  $\sigma_{*} - L_R$  fit given by B06 (their Figure 6 with colors of V-R=0.6 and R-K=3.0). We find shallower slopes for the E/S0 population consistent with B06. Figure 4(a) demonstrates that the “bending” of the  $\sigma_{*} - L_V$  relation, as noted by B06, is also seen in the L06 sample; BCGs fall above the relation defined by the E/S0s. In the NIR (Figure 4b) the BCGs do not appear to define a separate population; instead their distribution is indistinguishable from that of the E/S0s. The average offset of BCGs from the E/S0 relation is 1.20 mags in  $M_V$  and 0.48 mags in  $M_K$ .

Figure 5 presents the relationship between  $M_{\bullet}$  estimated from the V-band (hereafter  $M_{\bullet}(V)$ ), using the relation as defined by L06 (their Equation 4), and  $M_{\bullet}$  estimated from the NIR data (hereafter  $M_{\bullet}(J, H, K)$ ) using the relations defined by the MH03 sample. The upper limit for  $M_{\bullet}(V)$  is  $10^{10.5} M_{\odot}$ . Below  $M_{\bullet} \approx 10^{8.5} M_{\odot}$  the agreement between all bands is good. Above  $10^{8.5} M_{\odot}$ , the NIR data predict significantly lower SMBH masses, with none exceeding  $10^{9.4} M_{\odot}$ . The fit to the K-band relation is shown as a dotted line and has a slope of  $0.62 \pm 0.02$  ( $0.74 \pm 0.02$  for E/S0s). For estimates of  $M_{\bullet}(J, H, K)$  we do not use the exact fits presented by MH03 (e.g. their Table 2) as they were derived using a bisector method (e.g., assuming scatter in both  $M_{\bullet}$  and  $L_{J,H,K}$ ). Instead,  $M_{\bullet}(J, H, K)$  has been determined from a single Y|X fit to  $M_{\bullet}$  and  $L$  (taking into account errors from both axis) because in estimating  $M_{\bullet}$  from  $L$  one assumes that all the scatter is in only one variable. The form of this relation, in the K-band, is given by  $\log M_{\bullet} = 8.22 \pm 0.07 + (1.06 \pm 0.11)(\log L_K - 10.9)$ . The results, in this case, are insignificant from the original MH03 fits ( $\sigma = 10^{0.04} M_{\odot}$ ).

Figure 6 shows how photometric  $M_{\bullet}$  estimates compare to those from the  $M_{\bullet} - \sigma_{*}$  relation. The Tremaine et al. (2002) expression is used to derive  $M_{\bullet}$  from  $\sigma_{*}$ , hereafter  $M_{\bullet}(\sigma_{*})$ . In Figure 6(a) the  $M_{\bullet} - L_V$  relation (above  $10^{8.5} M_{\odot}$ ) predicts SMBH masses greater than those expected from the  $M_{\bullet} - \sigma_{*}$  relation. However, in the NIR, this observation is not made; both predictions are consistent. The  $M_{\bullet} - L_V$  relation implies  $M_{\bullet} \lesssim 2.5 \times 10^{10} M_{\odot}$ , whereas the NIR produces  $M_{\bullet} \lesssim 2.8 \times 10^9 M_{\odot}$ . The scatter in the  $M_{\bullet}(J, H, K) - M_{\bullet}(\sigma_{*})$  relations are significantly less than the  $M_{\bullet}(V) - M_{\bullet}(\sigma_{*})$  relation.

The effect of the results from the § 2 simulations can be seen by artificially and randomly introducing the distribution of  $\Delta$  mag to the K-band magnitudes. A comparison of  $M_{\bullet}(\sigma_{*})$  and the adjusted  $M_{\bullet}(K)$  is shown in Figure 7. The slope of the best fit relation (dotted line) is  $0.85 \pm 0.05$  and no values of  $M_{\bullet}(K)$  exceed  $10^{9.7} M_{\odot}$ .

### 4. DISCUSSION

It is evident from both Figures 4 and 6 that the dispersion of BCGs in the NIR is considerably less than in the V-band. This is also the case for the E/S0s. Even if we are underestimating the NIR luminosities, it would require a very fortunate coincidence to have such a strong agreement between  $M_{\bullet}(\sigma_{*})$  and  $M_{\bullet}(J, H, K)$  across the entire mass function. It then follows that BCGs are not “special” when viewed at NIR wavelengths. BCGs follow the same  $\sigma_{*} - L_K$  distribution as defined by less luminous spheroids, and comparable masses are predicted for the SMBHs in BCGs based either on velocity dispersions or on total magnitudes.

We have demonstrated, through extensive simulations, that the 2MASS magnitudes used in this study are robust to within 0.5 mags for BCGs. This is consistent with the offset between the 2MASS photometry and that of MH03, who take the total magnitude components of Sérsic fits to two-dimensional photometric models. This offset is expected as the 2MASS total magnitude integrations stop at  $r_{\text{ext}}$ . For the  $M_{\bullet} - L_{J,H,K}$  relations to predict a population of  $10^{10} M_{\odot}$  SMBHs, i.e., for the BCGs to fall on the one-to-one relation in Figure 5, 2MASS photometry would have to be increased, on average, by 1.65 mags. This offset is inconsistent with the 2MASS underestimates. The offset would also need to vary with  $M_{\bullet}$  and have no effect at masses below  $10^{8.5} M_{\odot}$  where the results between  $M_{\bullet} - L_V$  and  $M_{\bullet} - L_{J,H,K}$  are consistent. Conversely, the V-band photometry must be overestimated by 2.17 mags, on average, for the upper limit of  $M_{\bullet}$  to be similar to that predicted from the NIR.

Why then do BCGs show an excess of V-band light over their less massive cousins? The issue could be resolved by considering the faint extended luminous halos known to surround the most massive galaxies (Oemler 1976). The signature of such halos is an inflection in the SBPs at large  $r$ . In the NIR, the total magnitudes could be missing the contributions from faint halos or, alternatively, V-band luminosities could be interpreted as over-estimates due to the spurious inclusion of halo light. Since extended halos predominantly sit in the overall cluster potential, they are unlikely to be related dynamically to the central regions from which the BCG  $\sigma_{*}$  is typically measured. Photometry from further toward the blue end of the spectrum may be deep enough to include a significant contribution from these extended halos, leading to an increase in the estimation of BCGs luminosities and a turn-over in  $M_{\bullet}$  estimates above a certain threshold.

While we have shown that BCGs are not “special” in terms of their  $\sigma_{*} - L_K$  distribution, nevertheless, their extreme luminosities and unique locations close to the centers of galaxy clusters suggest special formation processes. It has long been argued that the extended envelopes of BCGs are debris from tidally-stripped galaxies, and hence that they are associated more closely with the overall cluster potential well than with any single

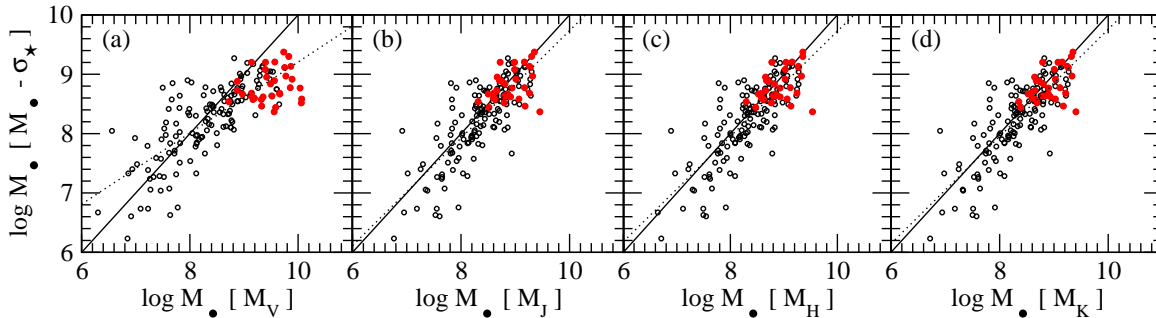


FIG. 6.— Comparing photometric  $M_{\bullet}$  estimates with  $M_{\bullet} - \sigma_{*}$  estimates. V, J, H and K masses (a, b, c and d respectively) are compared to  $M_{\bullet} - \sigma_{*}$  estimates. Open black circles are E/S0s, BCGs are filled red circles. In all cases the solid line represents a one-to-one relation and the dotted line the best-fit relation.

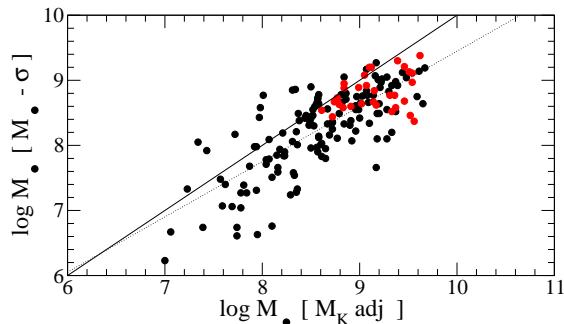


FIG. 7.— Comparing redistributed  $M_{\bullet}(K)$  estimates with  $M_{\bullet} - \sigma_{*}$  estimates. Black circles are E/S0s, BCGs are red circles. The solid line represents a one-to-one relation and the dotted line the best fit relation.

galaxy (Merritt 1984a). The envelopes may also consist in part of stars formed in cooling flows (Fabian 1994). The presence of multiple nuclei in some BCGs argues in favor of these galaxies not being fully relaxed (Merritt 1984b). A photometrically complete, high-resolution imaging survey of BCGs would be able to provide a framework for a more quantitative analysis of these fundamentally important objects.

## 5. CONCLUSIONS

Brightest cluster galaxies offer the chance to study the pinnacle of galaxy evolution. They also give us the opportunity to study the top of the SMBH food chain by using the observed relations between  $M_{\bullet}$  and the properties of the surrounding host galaxy. We have shown that NIR luminosities, combined with previously established scaling relations (MH03), imply a maximum mass of  $\sim 3 \times 10^9 M_{\odot}$ . This is consistent with the most

massive SMBH directly modeled at the center of M87 (Macchetto et al. 1997) and with the direct  $M_{\bullet}$  estimates of Dalla Bontá et al. (2006) in 3 BCGs. We also find that, across all values, SMBH masses predicted using NIR magnitudes are consistent with masses predicted from  $\sigma_{*}$ . In addition, we have shown that BCGs follow the same distribution, as defined by E/S0 galaxies, in the  $\sigma_{*} - L_K$  relation. If confirmed by a deep multiwavelength study, these findings could have important implications for the nature of the SMBH mass function, and, as in the past, would show that NIR data are to be preferred when estimating  $M_{\bullet}$  (MH03). While BCGs are likely not special – in the sense of hosting hyper-massive black holes or by defining a distinct population in the  $\sigma_{*} - L_K$  plane – they may be interesting by virtue of being surrounded by extended faint halos. The unique local BCG environment, deep within a cluster potential, could be the generator of these halos, which may be populated by younger stars tidally stripped from other cluster members or that are the results of intra-cluster gas accretion or other recent merger events.

We would like to thank Alister Graham, Tod R. Lauer and Mariangela Bernardi for their comments on this manuscript. This research used NASA/IPAC Infrared Science Archive, which is operated by the JPL, CalTech, under contract with the NASA. We acknowledge the usage of the HyperLeda database (<http://leda.univ-lyon1.fr>). D.M acknowledges support from grants AST 00-71099, AST 02-06031, AST 04-20920, and AST 04-37519 from the NSF, grant NNG04GJ48G from NASA, and grant HST-AR-09519.01-A from STScI.

## REFERENCES

- Andreon, S. 2002, *A&A*, 382, 495  
 Bernardi, M., et al. 2006, submitted (astro-ph/0607117)  
 Dalla Bontá, E., et al. 2006, in press (astro-ph/060702)  
 Fabian, A. C. 1994, *ARA&A*, 32, 277  
 Ferrarese, L., & Merritt, D. 2000, *ApJ*, 539, L9  
 Ferrarese, L., & Ford, H. 2005, *Space Science Reviews*, 116, 523  
 Gebhardt, K., et al. 2000, *ApJ*, 539, L13  
 Graham, A., Lauer, T. R., Colless, M., & Postman, M. 1996, *ApJ*, 465, 534  
 Graham, A. W., & Driver, S. P. 2007, *ApJ*, 655 (astro-ph/0607378)  
 Kormendy, J., & Richstone, D. 1995, *ARA&A*, 33, 581  
 Laine, S., van der Marel, R. P., Lauer, T. R., Postman, M., O’Dea, C. P., & Owen, F. N. 2003, *AJ*, 125, 478  
 Lauer, T. R., et al. 2006a, submitted (astro-ph/0606739)  
 Macchetto, F., Marconi, A., Axon, D. J., Capetti, A., Sparks, W., & Crane, P. 1997, *ApJ*, 489, 579  
 Marconi, A., & Hunt, L. K., 2003, *ApJ*, 589, L21  
 Merritt, D. 1984a, *ApJ*, 276, 26  
 Merritt, D. 1984b, *ApJ*, 280, L5  
 Oemler, A., Jr. 1976, *ApJ*, 209, 693  
 Paturel, G., Petit, C., Prugniel, P., Theureau, G., Rousseau, J., Brouty, M., Dubois, P., & Cambrésy, L. 2003, *A&A*, 412, 45  
 Peng, C. Y., Ho, L. C., Impey, C. D., & Rix, H.-W. 2002, *AJ*, 124, 266  
 Postman, M., & Lauer, T. R. 1995, *ApJ*, 440, 28  
 Schlegel, D. J., Finkbeiner, D. P., & Davis, M. 1998, *ApJ*, 500, 525  
 Sérsic, J. L. 1963, *Boletín de la Asociación Argentina de Astronomía La Plata Argentina*, 6, 41  
 Tonry, J. L., Dressler, A., Blakeslee, J. P., Ajhar, E. A., Fletcher, A. B., Luppino, G. A., Metzger, M. R., & Moore, C. B. 2001, *ApJ*, 546, 681  
 Tremaine, S., et al. 2002, *ApJ*, 574, 740